Lattice site and photoluminescence of erbium implanted in $\alpha-Al_2O_3$

G. N. van den Hoven and A. Polman
FOM-Institute for Atomic and Molecular Physics, Kruislaan 407, 1098 SJ Amsterdam, The Netherlands

E. Alves, M. F. da Silva, and A. A. Melo
Dep. de Física, ITN, Estrada National 10, P-2685 Sacavém, Portugal

J. C. Soares
Centro de Física Nuclear da Universidade de Lisboa, Av. Prof. Gama Pinto, 2, 1699, Lisboa Codex, Portugal

(Received 5 January 1996; accepted 2 November 1996)

Single-crystal sapphire ($\alpha-Al_2O_3$) was implanted at room temperature with 200 keV erbium ions to a fluence of 8×10^{13} cm^{-2}. Ion channeling using 1.6 MeV He^+ shows that the crystal suffers little damage for this low dose implant. Angular scans through axial and planar directions in the crystal indicate that 70% of the Er atoms reside on displaced octahedral sites in the $\alpha-Al_2O_3$ lattice. As pure Al_2O_3 has a high density of free octahedral sites, this explains why high concentrations of Er can be dissolved in this material. Smaller fractions of Er are found on tetrahedral (20%) and random (10%) sites. The samples exhibit strongly peaked photoluminescence spectra around 1.5 μm, due to intra-4*f* transitions in Er^{3+}, indicating the existence of well-defined sites for the luminescing Er^{3+} ions. It is concluded that the octahedral site is the dominating optically active site in the lattice.

I. INTRODUCTION

Rare earth doped optical waveguide materials are experiencing a strong development in the field of integrated optics because of their application as optical amplifiers and lasers. In particular, the rare earth ion Er^{3+} is of interest due to its intra-4*f* transitions around 1.54 μm, a standard telecommunications wavelength. Recently, high-quality, low-loss compact Al_2O_3 waveguide structures have been fabricated on Si substrates,[1,2] and doped with Er by ion implantation.[3] When optically pumped at 1.48 μm, these Al_2O_3 waveguide amplifiers show net optical amplification of a signal at 1.53 μm.[4] This result was achieved due to the fact that high concentrations of optically active Er could be dissolved in the Al_2O_3 lattice. The exact lattice location of Er in Al_2O_3, however, is still unknown.

Figure 1 shows the crystal structure of $\alpha-Al_2O_3$ (sapphire). The O atoms form a hexagonally close-packed lattice; the Al atoms occupy octahedral sites between the O planes. As for every three O atoms there are only two Al atoms, one out of three octahedral sites is empty. Since the Al atoms themselves form a regular structure, the octahedral sites occupied by Al are distinctly different from the free octahedral sites. Also indicated in the figure (for later reference) is a tetrahedral site; such sites are all unoccupied in the Al_2O_3 lattice.

The crystal structure of $\gamma-Al_2O_3$, the material used for Er-doped Al_2O_3 waveguide films, is similar to that of $\alpha-Al_2O_3$, but in this case the O atoms form a face-centered cubic structure. Er_2O_3 has essentially the same crystal structure as $\gamma-Al_2O_3$, but with Er instead of Al on octahedral sites.

In this work, the lattice site of Er-implanted sapphire (single-crystal $\alpha-Al_2O_3$) is investigated using ion-channeling techniques. Previously, we have studied the damage and annealing behavior of Er-implanted sapphire, and the results are reported in Ref. 5. In the present work, the Er is found to reside on displaced octahedral sites in the lattice, which are empty in undoped $\alpha-Al_2O_3$. It is found that this site is the dominant optically active site.

II. EXPERIMENTAL

Single crystal $\langle 0001 \rangle$ and $\langle 01\bar{1}0 \rangle$ oriented $\alpha-Al_2O_3$ wafers were implanted with 200 keV Er to a fluence of 8×10^{13} ions/cm^2 with the samples held at room temperature. The samples were tilted by 7° with respect to the ion beam to avoid channeling of the implanted ions. A $\langle 0001 \rangle$-oriented $\alpha-Al_2O_3$ sample was implanted with 5×10^{14} Er/cm^2 for photoluminescence spectroscopy measurements. The samples were not annealed.

Rutherford backscattering spectrometry (RBS)/ion channeling analysis was performed with 1.6 MeV He^+ ions accelerated using a Van de Graaff accelerator. The backscattered particles were detected by two surface barrier detectors, which were placed at 160° and close to

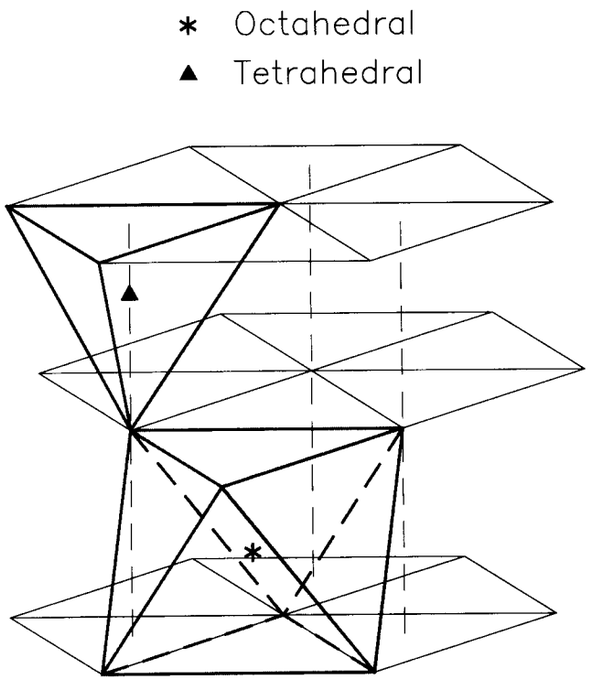

FIG. 1. Schematic of the crystal structure of $\alpha-Al_2O_3$ (sapphire). The O atoms form a hexagonal close-packed lattice indicated by the thin solid lines. At each intersection of these lines there is one O atom; the hexagons indicate the O planes. The Al atoms occupy octahedral sites; one of these is indicated in the figure. For every O atom there exists one octahedral site. Also indicated is a tetrahedral site. The vertical dashed lines indicate how the oxygen planes are stacked with respect to each other.

180° with respect to the incoming He^+ beam direction. The energy resolutions for these detectors were 14 and 18 keV, respectively. The samples were placed on a two-axis goniometer, enabling alignment of the crystal axes with the incoming He^+ beam. In addition, the samples could be continuously rotated around the sample surface normal in order to obtain true random spectra. The beam current was kept below 1 nA in a 0.4 mm^2 spot in order to prevent pileup of measurement pulses. Each measurement was done on a fresh spot. The spectra were recorded using a multichannel analyzer.

Photoluminescence (PL) measurements were performed at room temperature using the 488 nm line of an Ar ion laser as an excitation source. This wavelength excites Er^{3+} into the $^2H_{11/2}$ energy level, after which rapid, nonradiative decay to the first excited ($^4I_{13/2}$) state occurs.[6] Subsequently, radiative decay to the ground state can occur, giving rise to light emission around 1.53 μm. The pump power was 250 mW focused in a 0.1 mm diameter spot, and the beam was mechanically chopped at 15 Hz. Luminescence emitted by the sample was collected with a lens, and dispersed using a 48 cm single-grating monochromator. The luminescence was detected with a liquid-nitrogen-cooled germanium detector, and the signal was amplified using a lock-in technique.

III. RESULTS AND DISCUSSION

A. Ion channeling

Figure 2 shows the random and channeling RBS spectra of a ⟨0001⟩-oriented sapphire sample implanted at room temperature with 8×10^{13} Er/cm^2. For comparison, the channeling spectrum of an unimplanted sapphire sample is shown. It overlaps with that of the implanted sample except for the Er part, indicating that the implant has caused very little damage to the sapphire lattice. It is known that high implantation fluences are necessary to cause significant damage to Al_2O_3 crystal lattice.[7] Also, the minimum yield for the implanted Er is low, indicative of a high fraction of Er on regular positions in the sapphire lattice. Note that the sample has not been annealed after implantation.

Figure 3 shows normalized angular scans for the Al, O, and Er ions for three axial directions (⟨0001⟩, ⟨01$\bar{1}$0⟩, and ⟨11$\bar{2}$0⟩) and for the corresponding planar directions. The samples used for these measurements are ⟨0001⟩-oriented (for ⟨0001⟩, (10$\bar{1}$0), and (11$\bar{2}$0) measurements) and ⟨01$\bar{1}$0⟩-oriented (for (0001), ⟨01$\bar{1}$0⟩, and ⟨11$\bar{2}$0⟩ measurement). The dips in the scans are due to alignment of the incoming He^+ beam with crystallographic directions in the lattice. Figure 4 shows the projections of the Al, O, free octahedral, and tetrahedral sites, for the six alignment conditions used in our experiment. By

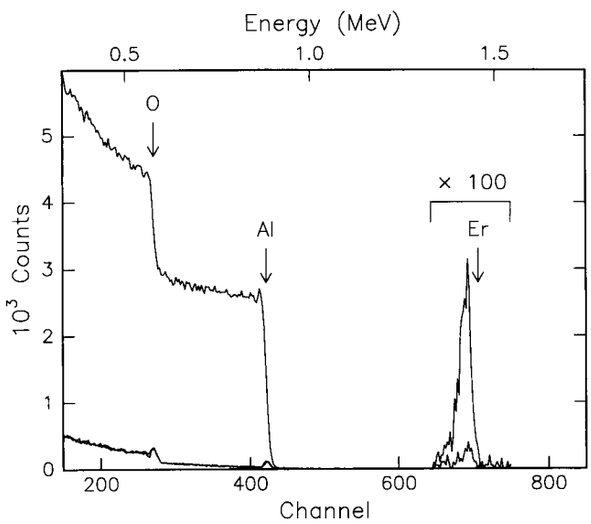

FIG. 2. RBS spectra of a ⟨0001⟩ oriented sapphire sample implanted with 8×10^{13} 200 keV Er/cm^2 at room temperature. A channeling spectrum (incoming beam in the ⟨0001⟩ direction) as well as a random spectrum are shown. For comparison, the channeling spectrum of an unimplanted sapphire sample is shown. It overlaps with that of the implanted sample, except for the Er part.

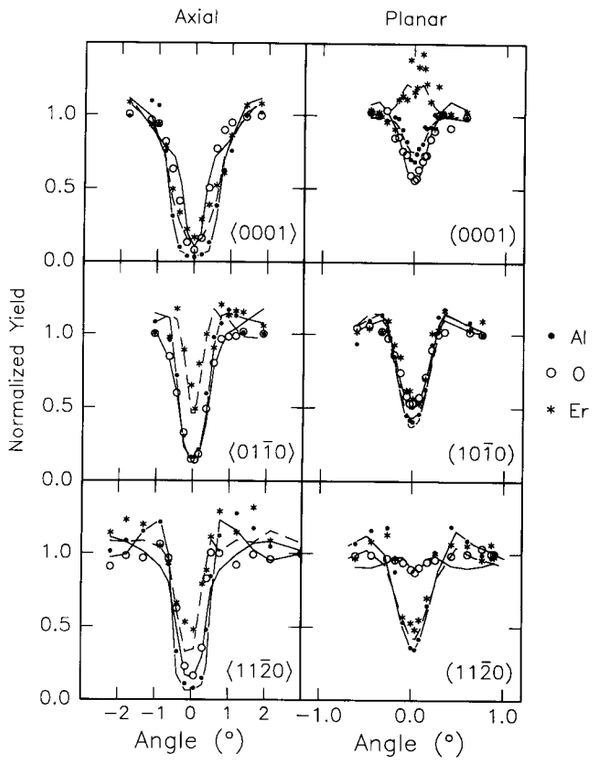

FIG. 3. Normalized angular scans for the Al, O, and Er ions for three axial directions (⟨0001⟩, ⟨01$\bar{1}$0⟩, and ⟨11$\bar{2}$0⟩) and for the corresponding planar directions. The samples were implanted with 8×10^{13} 200 KeV Er/cm^2. Simulations of the measured data are shown as drawn lines (Al and O: solid line; Er: dashed line).

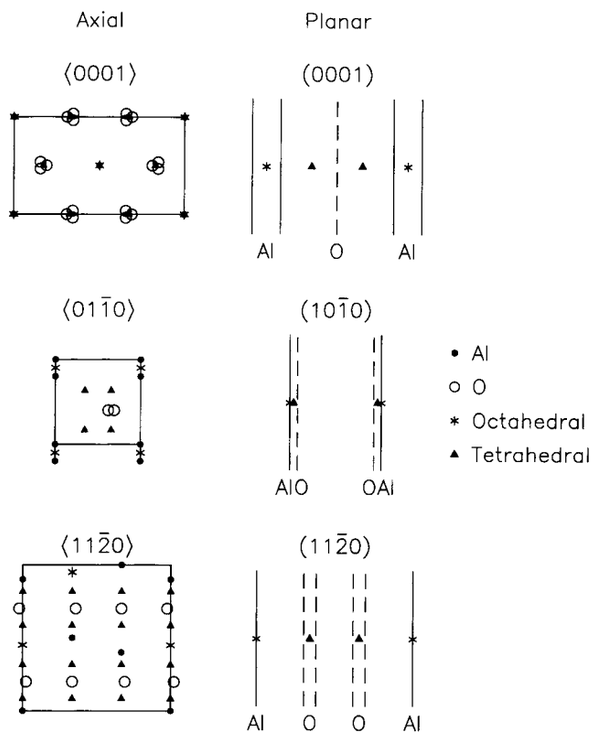

FIG. 4. Projections of the Al, O, free octahedral, and tetrahedral sites, in the crystal directions used for the angular scan measurements.

comparing the Er yield as a function of angle to the signals for Al and O for these six conditions, the Er lattice site can be determined unambiguously.

Figure 3 shows that for the (10$\bar{1}$0) and the (11$\bar{2}$0) planar directions, the Er yield overlaps very well with that of Al, whereas flux peaking for the Er is seen for the (0001) plane. In the ⟨0001⟩ axial direction the Er dip is centered at the same position as the Al dip, but does not reach the same minimum yield. In the ⟨01$\bar{1}$0⟩ and ⟨11$\bar{2}$0⟩ axial directions, the Er dips are less deep and narrower than those observed for Al and O. Clearly, the Er resides on regular sites in the Al_2O_3 lattice, but the differences in the angular scans show that these cannot be in either the Al or O sublattice.

Monte Carlo simulations of the angular scan data were performed in which the $\alpha-Al_2O_3$ crystal lattice was considered with Er atoms on different sites in the crystal structure. The code used for the simulations is reported elsewhere,[8] and was modified to simulate the $\alpha-Al_2O_3$ crystal lattice. Thermal vibration amplitudes of 0.087 Å, 0.067 Å, and 0.027 Å were taken for O, Al, and Er, respectively; these values were obtained using the Debye model with a Debye temperature of 950 K. Best agreement with the data was obtained by assuming that 70% of the Er occupies free octahedral sites (see Fig. 1), but displaced 0.8 Å along the ⟨0001⟩ direction from the ideal position. 20% of the Er is in tetrahedral sites (see Fig. 1), and the remaining 10% is randomly distributed. The results of the simulations for Al, O, and Er are included as drawn lines in Fig. 3. These results show that in $\alpha-Al_2O_3$, Er mainly occupies free octahedral sites, which have similar surroundings as Al and Er have in the $\alpha-Al_2O_3$ and Er_2O_3 crystal lattices, respectively. Note that the free octahedral sites are not identical to the octahedral sites occupied by Al.[9]

B. Photoluminescence

Figure 5 shows the room-temperature PL spectrum of Er-implanted sapphire (⟨0001⟩-oriented, 5×10^{14} Er/cm^2). The spectrum is typical for intra-4*f* transitions in Er^{3+},[6] and consists of a number of sharp lines, indicating that the luminescing Er^{3+} ions occupy well-defined sites in the $\alpha-Al_2O_3$ crystal. The spectral shape of the samples implanted at lower fluences is similar; however, the intensities are lower.

The luminescence intensity measured for the Er-implanted, $\alpha-Al_2O_3$ samples was compared to that of an Er-implanted, $\gamma-Al_2O_3$ waveguide film with a known amount of optically active Er. Assuming similar

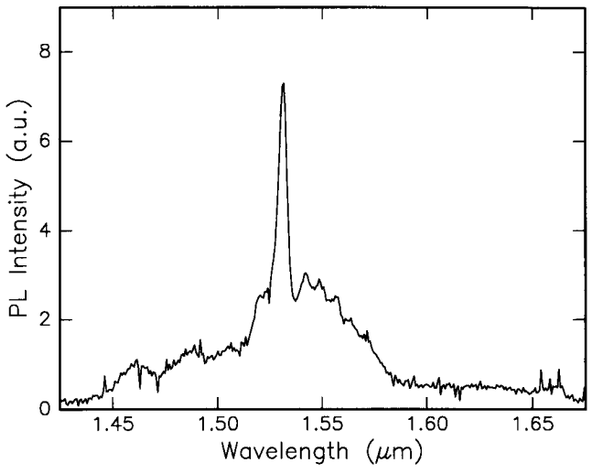

FIG. 5. Room temperature photoluminescence spectrum of ⟨0001⟩-oriented $\alpha-Al_2O_3$ implanted with 5×10^{14} 200 keV Er/cm^2. The excitation source was a 250 mW light beam at 488 nm from an Ar ion laser. The measurement resolution was 3 nm.

absorption and emission cross sections for Er^{3+} in these materials, this comparison indicates that on the order of 100% of the Er is optically active in the sapphire samples. As the previous section showed that most of the Er resides on octahedral positions in these samples, we conclude that Er on this octahedral site is indeed the luminescing Er. We cannot exclude the possibility that Er in tetrahedral sites or even on random positions also show luminescence; however, the octahedral site is the dominating luminescing site.

The results of this study can be used to explain why high amounts of optically active Er can be incorporated in Al_2O_3. In order to exhibit the characteristic radiative transitions around 1.5 μm, Er should be in the trivalent state. In the Al_2O_3 crystal, the Al atoms, with occupy octahedral sites, are also trivalent. Here it is found that Er occupies similar (free octahedral) sites, implying that it is indeed trivalent in the lattice. Furthermore, octahedral positions in the Al_2O_3 lattice have a 6-fold surrounding of O atoms. Such a surrounding for Er has been found previously to be optically active.[10] As one out of every three octahedral positions in the Al_2O_3 lattice are unoccupied, the effective solubility of Er in Al_2O_3 is high, and high amounts of optically active Er can be incorporated. Note that the above conclusions hold for both the hexagonal $\alpha-Al_2O_3$ lattice (sapphire) as well as the cubic $\gamma-Al_2O_3$ lattice (waveguide films), because the two lattices differ only in the stacking sequence of the O atoms, and have the same density of empty sites. Note that due to the implantation of Er in Al_2O_3, a surplus of cations is created. As a consequence, Al atoms may be forced to diffuse away in order to maintain charge neutrality. RBS data (not shown) indicate that Er itself does not diffuse during or after implantation at room temperature.

IV. CONCLUSIONS

In conclusion, the lattice site of Er implanted in sapphire ($\alpha-Al_2O_3$) is measured by ion-channeling; 70% is found on octahedral sites displaced by 0.8 Å along the ⟨0001⟩ direction, 20% resides on tetrahedral sites, the rest is randomly distributed. The samples exhibit photoluminescence at 1.5 μm, due to intra-4*f* transitions in Er^{3+}. Comparison of the luminescence intensities to those of Er-implanted, $\gamma-Al_2O_3$ waveguide films shows that on the order of 100% of the Er is optically active in sapphire. As most of the Er resides on displaced octahedral sites, it is concluded that this site is the dominating optically active site in the $\alpha-Al_2O_3$ lattice. The fact that pure Al_2O_3 has a high density of free octahedral sites can now explain why high amounts of optically active Er can be dissolved in the lattice.

ACKNOWLEDGMENTS

Work at the FOM-Institute is part of the research program of the Foundation for Fundamental Research on Matter (FOM), and was made possible by financial support from the Dutch Organization for the Advancement of Research (NWO), the IC Technology Program (IOP Electro-Optics) of the Ministry of Economic Affairs, and the Foundation for Technical Research (STW). This work has been partially funded by Junta Nacional de Investigação Científica e Tecnológica, Portugal through projects CERN/CA/982/92 and CA/1021/93.

REFERENCES

1. M. K. Smit, G. A. Acket, and C. J. van der Laan, Thin Solid Films, Electronics and Optics **138**, 171 (1986).
2. M. K. Smit, *Integrated Optics in Silicon-Based Aluminum Oxide,* Ph.D. Thesis, Optics Laboratory, Dept. of Applied Physics, Delft University of Technology (1991).
3. G. N. van den Hoven, E. Snoeks, A. Polman, J. W. M. van Uffelen, Y. S. Oei, and M. K. Smit, Appl. Phys. Lett. **62**, 3065 (1993).
4. G. N. van den Hoven, R. I. J. M. Koper, A. Polman, C. van Dam, J. W. M. van Uffelen, and M. K. Smit, Appl. Phys. Lett. **68**, 1886 (1996).
5. E. Alves, M. F. da Silva, G. N. van den Hoven, A. Polman, A. A. Melo, and J. C. Soares, Nucl. Instrum. Methods B **106**, 429 (1995).
6. S. Hüfner, *Optical Spectra of Transparent Rare-Earth Compounds* (Academic, New York, 1978).
7. C. W. White, C. J. McHargue, P. S. Sklad, L. A. Boatner, and G. C. Farlow, Mater. Sci. Rep. **4**, 41 (1989).
8. L. Rebouta, P. J. M. Smulders, D. O. Boerma, F. Agulló-López, M. F. DaSilva, and J. C. Soares, Phys. Rev. B **48**, 3600 (1993).
9. P. Villars and L. D. Calvert, *Pearson's Handbook of Crystallographic Data for Intermetallic Phases* (American Society for Metals, Metals Park, OH, 1986), pp. 1047, 2177, and references therein.
10. M. A. Marcus and A. Polman, J. Non-Cryst. Solids **136**, 260 (1991).